Mathematics

https://www.aimspress.com/journal/Math

AIMS Mathematics, 10(2): 2562–2588.
DOI: 10.3934/math.2025119
Received: 25 November 2024
Revised: 08 January 2025
Accepted: 10 January 2025
Published: 12 February 2025

Research article

Fractional derivatives, dimensions, and geometric interpretation: An answer to your worries

Abdon Atangana[1,2,3,*]

[1] Institute for Groundwater Studies, University of the Free State, South Africa, 205 Nelson Mandela Drive, 9301, South Africa

[2] Department of Medical Research,China Medical University Hospital,Taichung, Taiwan

[3] IT4Innovations, VSB-Technical University of Ostrava, Ostrava-Poruba, Czech Republic

* **Correspondence:** Email: AtanganaA@ufs.ac.za.

Abstract: In this study, I look into the study of fractional calculus in the mathematical modeling of nonlinear complex systems. I began by analyzing the dimensional aspects of fractional derivatives, in particular, the Caputo-Fabrizio and Atangana-Baleanu derivatives, and demonstrated that the fractional order can be interpreted as a distinct temporal dimension. Provided a thorough study of the mathematical kernels describing such derivatives, emphasizing their contrasting memory effects and the manner in which they impact the dynamics of the system. In particular, the Atangana-Baleanu derivative has the Mittag-Leffler kernel, which has smoother decay and is long-range compared to any power-law kernel or exponential kernels, with short-memory effects. Starting only from the energy and entropy responses related to each kernel, we showed how the fractional derivatives provide a more comprehensive description of the energy lost and the entropy gained. The kernels had stunning convolution properties that were analyzed to understand how the history and external heat effect the system dynamics via the kernel dependencies. As a new extension of artificial intelligence against DML, a novel method utilizing fractional calculus was proposed in LED lifespan modeling with varying ambient conditions. The model has been developed using several fractional kernels so that thermal cycling, humidity, mechanical stress, and electrical stress can be used to analyze and capture the degradation of the LED. The icing on the cake is that these fractional kernels inherently include memory effects and can be used to realistically and tailorably predict LED lifetime in a variety of environments. This study illustrates the possibility of using fractional derivatives framework to go beyond delivering physical understanding regarding time dependency of degradation processes.

Keywords: fractional derivatives; Caputo-Fabrizio; Atangana-Baleanu; LED lifespan; energy dynamics; entropy; memory effects
Mathematics Subject Classification: 00A73, 26A33, 34A08

1. Introduction

In general, it is known that the concept of fractional calculus has been developed intensively since the fundamental worries of Gottfried Leibniz and Bernard L'Hopital. Even though their focus was on derivatives with integer numbers, and their explorations led to a fascinating question: What if $n = \frac{1}{2}$? This inquiry toward derivatives with non-integer orders opened doors to a realm of fractional calculus, a concept that has challenged the conventional understanding of differentiation and integration. Indeed, at the heart of this realm lies a paradox answered by Leibniz. The definition of classical derivative assumes the continuity and smoothness that may not be true for fractional derivatives. A clear example is the case of the Riemann-Liouville, where the function only needs to be continuous [1]. The implication of this paradox extends to the concept of dimension and geometric interpretation [2]. However, in fractional calculus, the dimension of a derivative is not always an integer, which is very strange and unacceptable for those that do not connect to the realm of fractional calculus. However, this leads to richer but more complex frameworks for the analysis of dynamical systems. Again, the concept of geometry becomes highly important. One should note that the fractional derivatives based on the power-law [1], for example, can be viewed through fractional laws, where the space is characterized by non-integer dimensions. Thus, this enriches our understanding of physical phenomena. We present some examples to underpin the argument. Let us assume that for an athlete to get a contract, we perform consistently in two different sport and the final records will be communicated to the contractor. Last the athlete ran a distance of 50 km flat terrain and scored an average speed of 20 km/h. Second event, the athlete ran the same distance but this time the terrain had a slope of 45 degrees and scored 5 km/h. The two scores are sent to the contractor, though the information about the terrain is not revealed. The question here is concept of speed work here? Can the expressions of $\frac{\Delta x}{\Delta t}$ scores be used to evaluate the athlete? The external forces here are not mentioned.

The use of power-law in modeling nature powers for example diffusion and reaction kinetics provides insight into the behavior of systems in the classical linear models that fall short. It should be noted that the power-law function reveals self-similarity and scale invariances as these properties make this function important in different fields of physics and social sciences, to mention a few. The exponential function serves as a main tool in modeling decay processes [3]. Similarly, the Mittag-Leffler function which is the generalization of the exponential function, captures the intricacies of anomalous diffusion, with application in many fields of science, engineering, and technology [4].

Fractional derivatives, in some cases, can be viewed as convolution of classical derivatives and kernels. In this case, central to these debates is the concept of convolution, and I note that a convolution is a mathematical operator that combines two functions to produce a third function. Convolution is verifying instrumentals in modeling processes in signal processing, image processing, chemistry, and system analysis [5]. This enables us to understand the cumulative effect of inputs over time. Thus, within the realm of fractional calculus, convolution takes or adds importance, in particular when the exploration of the application of fractional derivatives is concerned. The convolution of two functions and areas under curves are simulated in Figure 1.

Indeed, the concept of first derivative is the base of differential calculus, which defines the rate of change of a given function, helping us understand the variation of such function as time or space. Now, within the framework of fractional calculus, the concept of first derivative is extended to understand change in non-integer dimensions. The convolution of the first derivative with kernels such as exponential, Mittag-Leffler, and power-law, provides a unique insight into system dynamics. The convolution of the first derivative with an exponential function results in a specific memory in which past states exponentially influence future behavior. This leads to a rapid decay in influence over time, this can be referred to as fading memory. Conversely, the convolution of a first derivative with power-law kernel leads to a long-range correlations, where the impact of the past events reduces more slowly, characterizing the persistent effects often observed in many complex systems. The convolution of the Mittag-Leffler kernel with the first derivative offers a versatile framework that replicates a blend of both exponential and power-law behaviors. This enables a nuanced modeling of phenomena, exhibiting both rapid and slow decays, which is an indicator of crossover.

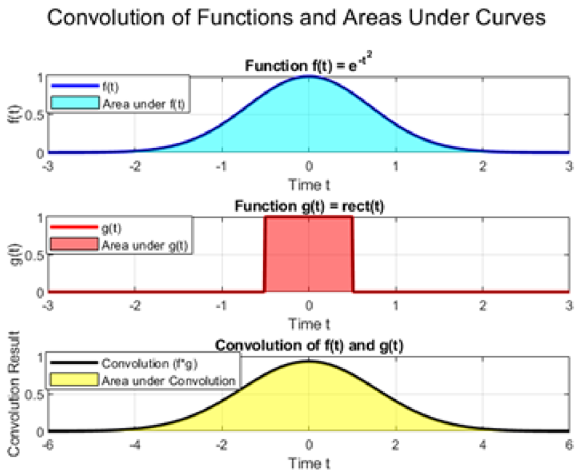

Figure 1. Convolution of the functions f and g.

In recent decades, the notion of dimension of fractional derivatives together with their geometrical interpretation have attracted the attention of several scholars from different backgrounds. Therefore, together, these explorations into fractional differential calculus, dimensionality, and convolution reveal the paradox implication of the discussion set by Leibniz and L'Hopital. I aim to set the change for a deeper examination of how these concepts interplay in applications, increase our understanding of both applications and theory. I provide a comprehensive analysis that addresses concerns raised by non-specialists in fractional calculus.

2. Definitions and dimensions

In exploring the dimensions, geometric interpretation of fractional derivatives is needed. I first present definitions of some fractional differential calculus and the dimension of some values. Moreover, I present the dimensions of some commonly used quantities:

a) Time $[T]$ (seconds);
b) Position $[L]$;
c) Velocity $V = \frac{dx}{dt}$, $\left[LT^{-1}\right]$ (m/s);
d) Acceleration $a = \frac{d^2x}{dt^2}$, $\left[LT^{-2}\right]$ (m/s^2);
e) Diffusion coefficient $\left[L^2T^{-1}\right]$ (m^2/s);

f) Force T, $\left[MLT^{-2}\right]$;
g) Energy E, $\left[ML^{2}T^{-2}\right]$;
h) Viscosity M $\left[ML^{-1}T^{-1}\right]$;
i) Concentration $\left[ML^{-3}\right]$.

2.1. Definitions of fractional derivatives

Let f be a function continously differentiable,

$$ {}_{t_0}^{C}D_t^{\alpha} f(t) = \int_{t_0}^{t} \frac{(t-\tau)^{-\alpha}}{\Gamma(1-\alpha)} f'(\tau)\, d\tau, \tag{2.1} $$

$$ {}_{t_0}^{CF}D_t^{\alpha} f(t) = \frac{1}{1-\alpha} \int_{t_0}^{t} f'(\tau) \exp\left(-\frac{\alpha}{1-\alpha}(t-\tau)\right) d\tau, \tag{2.2} $$

$$ {}_{t_0}^{ABC}D_t^{\alpha} f(t) = \frac{1}{1-\alpha} \int_{t_0}^{t} f'(\tau) E_{\alpha}\left(-\frac{\alpha}{1-\alpha}(t-\tau)^{\alpha}\right) d\tau. \tag{2.3} $$

However, if f is continuous, we have

$$ {}_{t_0}^{RL}D_t^{\alpha} f(t) = \frac{d}{dt} \int_{t_0}^{t} \frac{(t-\tau)^{-\alpha}}{\Gamma(1-\alpha)} f(\tau)\, d\tau, \tag{2.4} $$

$$ {}_{t_0}^{CF}D_t^{\alpha} f(t) = \frac{1}{1-\alpha} \frac{d}{dt} \int_{t_0}^{t} f(\tau) \exp\left(-\frac{\alpha}{1-\alpha}(t-\tau)\right) d\tau, \tag{2.5} $$

$$ {}_{t_0}^{ABC}D_t^{\alpha} f(t) = \frac{1}{1-\alpha} \frac{d}{dt} \int_{t_0}^{t} f(\tau) E_{\alpha}\left(-\frac{\alpha}{1-\alpha}(t-\tau)^{\alpha}\right) d\tau, \tag{2.6} $$

where $0 < \alpha < 1$. I note that ${}_{t_0}^{ABC}D_t^{\alpha} f(t)$ is the Atangana-Baleanu fractional derivative of f in Caputo sense. ${}_{t_0}^{ABR}D_t^{\alpha} f(t)$ is the Atangana-Baleanu fractional derivative of f in Riemann-Liouville sense. ${}_{t_0}^{C}D_t^{\alpha} f(t)$ is the Caputo fractional derivative. ${}_{t_0}^{CF}D_t^{\alpha} f(t)$ is the Caputo-Fabrizio fractional derivative. Here, Mittag-Leffler and exponential functions are defined as

$$ E_{\alpha}(-\lambda t^{\alpha}) = \sum_{j=0}^{\infty} \frac{(-\lambda t^{\alpha})^{j}}{\Gamma(\alpha j + 1)}, \tag{2.7} $$

and

$$ \exp(-\lambda t) = \sum_{j=0}^{\infty} \frac{(-\lambda t)^{j}}{j!}. \tag{2.8} $$

${}_{t_0}^{RL}D_t^{\alpha} f(t)$ is the Riemann-Liouville fractional derivative.

3. Dimension of fractional derivatives

I recall that dimensions are measurements of the space or environment in which entities exist, for example, width, length, height [2]. However, in a more abstract sense, they can represent different properties like time and concentration. Nevertheless, when dealing with fractional derivatives, dimensions get more intriguing. Fractals are examples of fractional dimensions. Thus, they can replicate the properties between convention dimensions, such as lines that are not really lines, surfaces that are not quite surfaces. It can be concluded that fractal dimensions help us model complex, irregular shapes observed in nature. Let $f(t)$ be a quantity with dimension $[f]$,

$$\left[\frac{df}{dt}\right] = [f]\left[T^{-1}\right]. \tag{3.1}$$

The above implies that the first derivative does not preserve dimensions.

$$\left[{}_{t_0}^{C}D_t^{\alpha} f(t)\right] = \left[\int_{t_0}^{t} \frac{(t-\tau)^{-\alpha}}{\Gamma(1-\alpha)} f'(\tau)\, d\tau\right] = [T^{-\alpha}]\,[f]\,[T]\left[T^{-1}\right]. \tag{3.2}$$

Therefore, the dimension of a Caputo derivative of f is $[f]\,[T^{-\alpha}]$. This is obtained since

$$\begin{aligned} [d\tau] &= [T], \\ [(t-\tau)^{-\alpha}] &= [T^{-\alpha}], \\ \left[\frac{df}{dt}\right] &= [f]\left[T^{-1}\right]. \end{aligned} \tag{3.3}$$

The dimension of a Riemann-Liouville derivative is found as

$$\begin{aligned} \left[{}_{t_0}^{RL}D_t^{\alpha} f(t)\right] &= \left[\frac{d}{dt}\int_{t_0}^{t} \frac{(t-\tau)^{-\alpha}}{\Gamma(1-\alpha)} f(\tau)\, d\tau\right] \\ &= \frac{\left[\int_{t_0}^{t} (t-\tau)^{-\alpha} f(\tau)\, d\tau\right]}{[T]} = \frac{[f]\,[T^{-\alpha}]\,[T]}{[T]} = [f]\,[T^{-\alpha}]. \end{aligned} \tag{3.4}$$

which gives the same dimension as in the case of Caputo derivative.

Before presenting the dimension of Caputo-Fabrizio and the Atangana-Baleanu derivatives, I shall first address the dimension of $E_{\alpha}(-t^{\alpha})$ and $\exp(-t)$. It is a very well-known fact that the arguments of any of the standard mathematical functions, such as trigonometric functions, logarithms, or exponentials that appear in the equation, must be dimensionless. As they require pure numbers as inputs and produce pure numbers as outputs. For example, the solution of the decay processes with fading memory

$$C(t) = C(0)\exp(-\lambda t). \tag{3.5}$$

$\exp(-\lambda t)$ expresses the fading memory that drives the decay. On one hand, the concentration $C(t)$ dimension is known but on the other hand, we have $C(0)\exp(-\lambda t)$ for the dimensions to balance, $\exp(-\lambda t)$ should be dimensionless. I note here that the above solution satisfies the equation

$$C'(t) = -\lambda C(t). \tag{3.6}$$

For a more complex decay, we have fast decay then a slow decay presenting a long tailed. This can be replicated using

$$C(t) = C(0) E_\alpha(-\lambda t^\alpha). \tag{3.7}$$

Here, $C(t)$ has the same dimension as $C(0)$. $E_\alpha(-\lambda t^\alpha)$ is the representation of the fast and slow decays, that is to say the function $E_\alpha(-\lambda t^\alpha)$ is the driving force of the decay. For the dimension to be balanced, we need $E_\alpha(-\lambda t^\alpha)$ dimension to be 1, particularly if $\lambda = 1$, so it holds. We note, however, that $C(0) E_\alpha(-\lambda t^\alpha)$ is the solution of the following equation

$$ {}_{t_0}^{C}D_t^\alpha C(t) = -\lambda C(t). \tag{3.8}$$

Let us now present the dimension of the Atangana-Baleanu and the Caputo-Fabrizio derivatives.

$$\begin{aligned} \left[{}_{t_0}^{ABC}D_t^\alpha f(t)\right] &= \left[\frac{1}{1-\alpha}\int_{t_0}^{t} f'(\tau) E_\alpha\left(-\frac{\alpha}{1-\alpha}(t-\tau)^\alpha\right)d\tau\right] \\ &= \left[\frac{1}{1-\alpha}\right][f]\left[T^{-1}\right][T] = \left[\frac{1}{1-\alpha}\right][f]. \end{aligned} \tag{3.9}$$

We have the above result since

$$\left[E_\alpha\left(-\frac{\alpha}{1-\alpha}(t-\tau)^\alpha\right)\right] = 1. \tag{3.10}$$

Therefore, the dimension of ${}_{t_0}^{ABC}D_t^\alpha f(t)$ is$\left[\frac{1}{1-\alpha}\right][f]$. Similarly,

$$\begin{aligned} \left[{}_{t_0}^{CF}D_t^\alpha f(t)\right] &= \left[\frac{1}{1-\alpha}\int_{t_0}^{t} f'(\tau) \exp\left(-\frac{\alpha}{1-\alpha}(t-\tau)\right)d\tau\right] \\ &= \left[\frac{1}{1-\alpha}\right][f]\left[T^{-1}\right][T] = \left[\frac{1}{1-\alpha}\right][f]. \end{aligned} \tag{3.11}$$

It appears that the Caputo-Fabrizio and the Atangana-Baleanu fractional derivatives have the same dimension, $\left[\frac{1}{1-\alpha}\right][f]$.

Here, the $\frac{1}{1-\alpha}$ factor becomes very important.Its dimension will lead to a clear physical interpretation of the fractional order α. The dimension of $\frac{1}{1-\alpha}$ in the case of both derivatives is $\left[T^{-1}\right]$, that is to say, the dimension of α in the case of both derivatives is $[T]$ such that

$$\left[{}_{t_0}^{ABC}D_t^\alpha f(t)\right] = \left[{}_{t_0}^{CF}D_t^\alpha f(t)\right] = \frac{[f]}{[T]}. \tag{3.12}$$

The above clearly leads us to the following physical interpretations: α, in the case of the Caputo-Fabrizio and the Atangana-Baleanu fractional derivatives, is a fraction of time. The full physical interpretation will be presented. The summary is presented in Table 1 below.

Table 1. Kernels and their dimensions.

Function	Convolution	Dimension
$\frac{1}{1-\alpha}\exp\left(-\frac{\alpha}{1-\alpha}t\right)$	${}_{0}^{CF}D_{t}^{\alpha}f(t)$	$[f]\left[T^{-1}\right]$
$\frac{t^{-\alpha}}{\Gamma(1-\alpha)}$	${}_{0}^{C}D_{t}^{\alpha}f(t)$	$[f]\left[T^{-\alpha}\right]$
$\frac{1}{1-\alpha}E_{\alpha}\left(-\frac{\alpha}{1-\alpha}t^{\alpha}\right)$	${}_{0}^{ABC}D_{t}^{\alpha}f(t)$	$[f]\left[T^{-1}\right]$

I shall provide dimension of fractal [6] and fractal-fractional differential operators [7].

$$\left[\frac{df}{dt^{\beta}}\right]=\frac{[f]}{[T^{\beta}]}. \tag{3.13}$$

This shows that the dimension of a fractal derivative is the same with that of a power-law based fractional derivative. For a fractal-fractional derivative with exponential function, we have

$$\begin{aligned}\left[{}_{0}^{FFE}D_{t}^{\alpha,\beta}f(t)\right] &= \left[\frac{1}{1-\alpha}\right]\left[\frac{d}{dt^{\beta}}\int_{0}^{t}f(\tau)\exp\left(-\frac{\alpha}{1-\alpha}(t-\tau)\right)d\tau\right] \\ &= \left[\frac{1}{T}\right]\frac{1}{[T^{\beta}]}[f][T]=\frac{[f]}{[T^{\beta}]}.\end{aligned} \tag{3.14}$$

For a fractal-fractional with power-law, we get

$$\left[{}_{0}^{FFP}D_{t}^{\alpha,\beta}f(t)\right]=\left[\frac{1}{\Gamma(1-\alpha)}\frac{d}{dt^{\beta}}\int_{t_0}^{t}(t-\tau)^{-\alpha}f(\tau)\,d\tau\right]=\frac{[T^{-\alpha}][f][T]}{[T^{\beta}]}=\frac{[f]}{[T^{\alpha+\beta-1}]}. \tag{3.15}$$

For a fractal-fractional with Mittag-Leffler, we have

$$\begin{aligned}\left[{}_{0}^{FFM}D_{t}^{\alpha,\beta}f(t)\right] &= \left[\frac{1}{1-\alpha}\frac{d}{dt^{\beta}}\int_{t_0}^{t}f(\tau)E_{\alpha}\left(-\frac{\alpha}{1-\alpha}(t-\tau)^{\alpha}\right)d\tau\right] \\ &= \left[\frac{1}{1-\alpha}\right]\frac{[f][T]}{[T^{\beta}]}=\frac{[f]}{[T]}\frac{[T]}{[T^{\beta}]}=\frac{[f]}{[T^{\beta}]}.\end{aligned} \tag{3.16}$$

In the next section, I shall provide some useful interpretation that will help explain the fundamental difference between these operators.

4. Interpretation of the obtained dimension and α

$$\left[{}_{0}^{CF}D_{t}^{\alpha}f(t)\right]=\left[{}_{0}^{ABC}D_{t}^{\alpha}f(t)\right]=\frac{[f]}{[T]}. \tag{4.1}$$

This shows that both differential operators retain the original quantity or derivative of the function. In the case of Caputo, there is an introduction of a scaling in the form of $[T^{-\alpha}]$ as power, with the of function $f(t)$. Therefore, fitting models only needed when there is a slow down because of memory. This can be observed in processes like diffusion in complex media. Here, from the above result, one can conclude that the dimensions balance in the case of Caputo-Fabrizio, Atangana-Baleanu, and Caputo, providing flexibility. The Atangana-Baleanu and the Caputo-Fabrizio maintain the conventional time-based scaling, and the Caputo can slow the rate of change, which is also used to replicate fractional dynamics.

4.1. *Immediate interpretation of* $\left[\frac{1}{1-\alpha}\right] = \left[\frac{1}{T}\right]$

I now provide an interpretation of α due to the relationship of the dimension of $\left[\frac{1}{1-\alpha}\right] = \left[T^{-1}\right]$. With this, the fractional order will be considered a measure of the extent of memory or the persistence in the dynamic of the system.

1) When α is near zero, factor $\frac{1}{1-\alpha}$ becomes smaller, which implies a significant memory effect, that the memory effects are weaker, and decay is faster. This could be translated into a more immediate response where past state events have less impact on the current state. The variation of the function with respect to α is present in Figure 2 below.

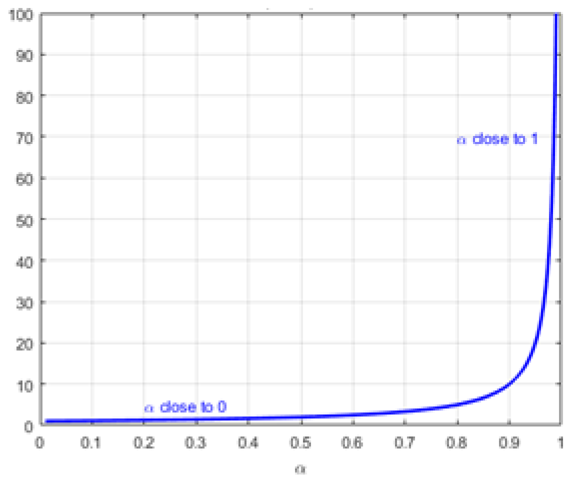

Figure 2. Scaling of α.

2) When α is closer to 1, the factor grows very large, revealing a stronger memory effect and slower decay. This leads to the system retaining more information from the past with an important persistence effect.

- α, therefore, acts as a rate modulator. This means α adjusts how fast, slow the influence of the past events reduces as a function of time. This has an impact on the system's dynamic memory properties.
- α can represent the degree of temporal decay. For example, when dealing with a system exhibiting fractional damping (viscoelastic materials), α will correspond to how elastic or viscous the feedback over time is, controlling how strain or stress vanishes.
- α is a temporal scale of the process. Because α is a time-relaxed dimensional influence, it ties fractional derivatives more closely to the property of time scales of the real-world problem.

Indeed, different values of α will relate to different processes. For instance, smaller α might be used to model processes in biology, geological diffusion, and others where there is slow or memory-intensive. Moreover, larger α could be used to replicate processes with less memory like some fluid dynamics. This results in process akin to conventional diffusion but prolonged, even if it excessively persistent memory effect. On the other hand, when the scaling factories are smaller, this could dampen the memory effect somewhat. However, the Mittag-Leffler kernel will decay very slowly, leading to a more slow reduction over time, but capturing a situation where the influence of the past events decays very is often observed in anomalous diffusion. In Table 2, below, we present a summary comparison.

Table 2. The comparison of the fractional derivatives.

Derivative	Role of α	Advantages	Disadvantages
Caputo	Power-law	Long memory, slow dynamic, easy to implement	nonlocal memory, fixed power-law kernel
Caputo-Fabrizio	Exponential decay	Fast decaying, smooth, stable	Limited long-range memory
Atangana-Baleanu	Mittag-Leffler	Balanced memory, adaptable, realistic decay	Newer with fewer tools

The graphical representation is depicted in Figure 3 below.

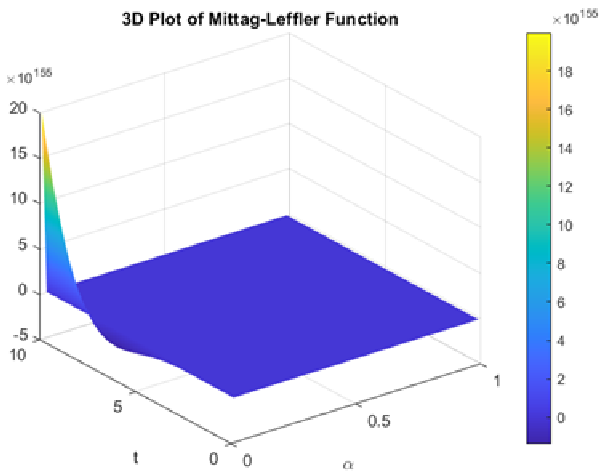

Figure 3. 3D graph of Mittag-Leffler function.

Therefore, this provides a long-term power-law decay, maintaining memory over a prolonged period. Therefore, the Mittag-Leffler kernel could be useful for replicating fast decay or heavy tailed memory effects in complex or fractal environments.

When $\frac{1}{1-\alpha}$ acts on $\exp\left(-\frac{\alpha}{1-\alpha}t\right)$, the product serves as a bridge between two types of decay and memory behaviors, this depends on the order α. Now, when $\alpha \to 1$, the prefactor $\frac{1}{1-\alpha}$ becomes larger, meaning exponential decay since $\exp\left(-\frac{\alpha}{1-\alpha}t\right)$ will drop rapidly. Therefore, the product decays to near zero values for a large time. Therefore, past states have a small influence, causing the behavior to be similar to conventional diffusion that dissipates rapidly. Thus, $\alpha \to 1$ leads to classical dynamics with almost no memory retention. When $\alpha \to 0$, factor $\frac{1}{1-\alpha}$ is smaller here, the product produces a gradual decrease, indicating a retention of fast events. Here, the past influence persists over time, which serves to model complex and long-memory process, though not like in the case of Mittag-Leffler kernel. In conclusion, this product smoothly interpolates between classical behavior with almost no memory for a larger α with memory-rich, slow decaying behavior when α is smaller. This makes the product a powerful tool in modeling diffusion and describing memory-driven phenomena arising in many fields. The graphical representation are depicted in Figures 4–6 below.

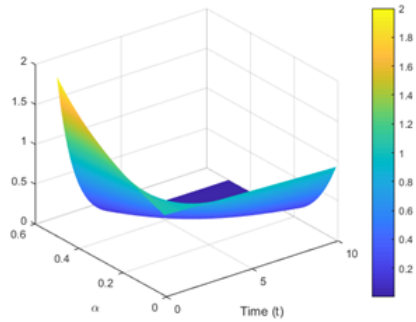

Figure 4. The graphical representation of exponential decay.

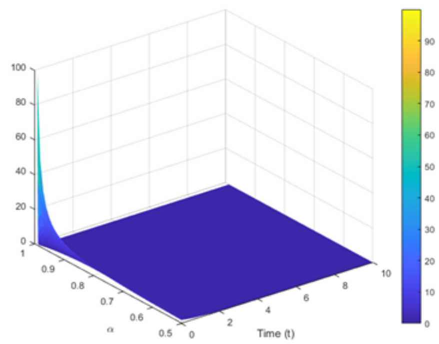

Figure 5. The graphical representation of exponential decay kernel.

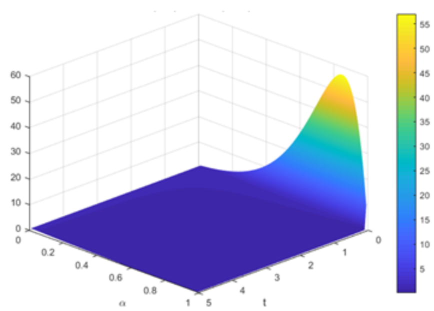

Figure 6. The graphical representation of power-law kernel.

I shall now present the summary in the below Table 3.

Table 3. Kernel analysis.

Aspect	$\frac{1}{1-\alpha}\exp\left(-\frac{\alpha}{1-\alpha}t\right)$	$\frac{1}{1-\alpha}\mathbf{E}_{\alpha}\left(-\frac{\alpha}{1-\alpha}t\right)$	$\frac{t^{-\alpha}}{\Gamma(1-\alpha)}$
Decay rate	Rapid decay, decay faster than both Mittag-Leffler and power-law	Intermediate decay, decays slower than exponential but faster than power at the origin	Slow decay: retains a long influence decaying, power than exponential and Mittag-Leffler kernel
Response to changes	Intermediate response: quickly lose the impact of the past events	Moderate response: retains memory of past events for a moderate duration	Prolonged response: retains the impact of the past much longer, leading to slower response
Behavior as $\alpha \to 1$	Approximate classical diffusion with small memory effects decay remains rapid	Approaches classical behavior but retains some memory; slower decay then exponential	Approaches classical diffusion but slower decay, allowing system long-lasting influence of past events however, diverges when t is zero
Behavior as $\alpha \to 0$	Decay is very fast, past state have small to no effect	Long-term memory effects are must pronounced; replicates anomalous diffusion	Indicates very slow decayand enduring memory effect
Memory effects	Minimal memory, decays faster, adequate for cases where present state is predominant	Moderate memory crossover between immediate response and long-memory; good for anomalous diffusion	Significant memory; past events have a long-lasting effect on the current state
Applications	Best for systems requesting fast adjustment: For example typical diffusion or advection	Adequate for anomalous diffusion, phenomena with intermediate memory effects	Ideal for a long-memory system for those with strong, slow moving correlations

4.2. Laplace transform analysis

I aim to analyze the Laplace transform of these functions [8]. Note that transforming these functions into the Laplace space may provide information on how they handle frequencies, in particular, for α-dependent rates of decay and more importantly, the memory effects. Thus, an investigation of poles and residues for each function is undertaken. The result obtained may help us understand how faster each function attenuate different frequencies components. This is important for application about wave propagation or signal processing.

$$L\left(\frac{1}{1-\alpha}\exp\left(-\frac{\alpha}{1-\alpha}t\right)\right) = \frac{1}{1-\alpha}\frac{1}{s+\frac{\alpha}{1-\alpha}} = \frac{1}{(1-\alpha)s+\alpha}, \tag{4.2}$$

and

$$F(s) = \frac{1}{(1-\alpha)s+\alpha}. \tag{4.3}$$

The pole of $F(s)$ occurs at

$$s = -\frac{\alpha}{1-\alpha}. \tag{4.4}$$

As $\alpha \to 1$, the pole is a larger negative value, which implies faster decay and a very weak memory effect.

When $\alpha \to 0$, the pole moves very close to zero. This shows that there is a slower decay rate in time domain, which implies more memory but not like in the case of power-law and Mittag-Leffler. For the power-law kernel, I have

$$L\left(\frac{t^{-\alpha}}{\Gamma(1-\alpha)}\right) = s^{\alpha-1} = F(s). \tag{4.5}$$

When

$$\lim_{\alpha\to 0} F(s) = \frac{1}{s}, \tag{4.6}$$

the pole is zero which implies a long-term memory effect. This is related to a persistent long-range dependency heavy-tailed behavior in time. Thus, this aligns with the understanding of anomalous diffusion where the effect of initial condition does not dissipate.

When $\alpha \to 1$, $F(s) = 1$, which is the Laplace of Dirac-delta, it indicates classical behavior. For the Mittag-Leffler, I have

$$L\left(\frac{1}{1-\alpha}E_\alpha\left(-\frac{\alpha}{1-\alpha}t^\alpha\right)\right) = \frac{1}{1-\alpha}\frac{s^{\alpha-1}}{s^\alpha+\frac{\alpha}{1-\alpha}} = \frac{s^{\alpha-1}}{(1-\alpha)s^\alpha+\alpha} = F(s). \tag{4.7}$$

When

$$\lim_{\alpha\to 1} F(s) = 1 = L(\delta(t)), \tag{4.8}$$

I have classical behavior. When

$$\lim_{\alpha\to 0} F(s) = \frac{1}{s}, \tag{4.9}$$

the pole is $s = 0$ the interpretation follows. If $0 < \alpha < 1$,

$$\alpha \quad > \quad 0 \Rightarrow \frac{1}{s^{1-\alpha}\left(s^\alpha+\frac{\alpha}{1-\alpha}\right)} \tag{4.10}$$

$$\Rightarrow \quad s = 0 \text{ and } s^{\alpha} = -\frac{\alpha}{1-\alpha}$$
$$\Rightarrow \quad s = 0 \text{ and } s = \left(-\frac{\alpha}{1-\alpha}\right)^{\frac{1}{\alpha}}.$$

I present the summary in Table 4 below.

Table 4. Laplace transform analysis of kernels.

Function	Laplace transform	Memory effect	Decay behavior
$\frac{1}{1-\alpha}\exp\left(-\frac{\alpha}{1-\alpha}t\right)$	$\frac{1}{(1-\alpha)s+\alpha}$	Weak for $\alpha \to 1$ strong for $\alpha \to 0$	Slower decay for $\alpha \to 1$ Fast decay $\alpha \to 0$
$\frac{t^{-\alpha}}{\Gamma(1-\alpha)}$	$s^{\alpha-1}$	Strong long-range memory	Slower decay
$\frac{1}{1-\alpha}E_{\alpha}\left(-\frac{\alpha}{1-\alpha}t^{\alpha}\right)$	$\frac{s^{\alpha-1}}{(1-\alpha)s^{\alpha}+\alpha}$	Balanced memory	Intermediate decay

5. Energy and entropy analysis

I present here a thorough energy and entropy analysis for each kernel [9]. I consider characteristics properties, and the result is analyzed within the framework of fractional calculus and anomalous diffusion. This helps in the analysis of each kernel, memory effects, and their respective behaviors over time having a focus on energy dimension and entropy.

For exponential kernels, the energy is given by

$$\begin{aligned} E_{\exp}^{CF} &= \int_0^{\infty}\left[\frac{1}{1-\alpha}\exp\left(-\frac{\alpha}{1-\alpha}t\right)\right]^2 dt = \frac{1}{(1-\alpha)^2}\int_0^{\infty}\left[\exp\left(-\frac{2\alpha t}{1-\alpha}\right)\right]dt \\ &= \frac{1}{2\alpha(1-\alpha)}, \end{aligned} \tag{5.1}$$

and I have

$$\lim_{\alpha\to 1} E_{\exp}^{CF} \to \infty. \tag{5.2}$$

This indicates high energy persistence for larger values of α. When

$$\lim_{\alpha\to 0} E_{\exp}^{CF} \to \infty. \tag{5.3}$$

This also indicates high energy influence because of small decay. For the case of power-law, I have

$$E_{power}^{C} = \int_0^{\infty}\left[\frac{t^{-\alpha}}{\Gamma(1-\alpha)}\right]^2 dt = \frac{1}{(\Gamma(1-\alpha))^2}\int_0^{\infty} t^{-2\alpha}dt. \tag{5.4}$$

However, the above could be investigated according to the range of α. Therefore, for $0 < \alpha < \frac{1}{2}$, I have

$$E_{power}(t,\alpha) = \int_{\varepsilon\to 0}^{\infty}\frac{t^{-2\alpha}}{\Gamma^2(1-\alpha)}dt = \lim_{\varepsilon\to 0}\frac{t^{1-2\alpha}}{\Gamma^2(1-\alpha)(1-2\alpha)}\Big|_{\varepsilon}^{\infty}. \tag{5.5}$$

Since $0 < \alpha < \frac{1}{2}$, I have a finite energy that is proportional to $\frac{1}{\Gamma^2(1-\alpha)(1-2\alpha)}$. The above will then help capture the extent and strength of memory. As $\alpha \to 0$, $\frac{1}{\Gamma^2(1-\alpha)(1-2\alpha)}$ is smaller. However, $\alpha \to \frac{1}{2}$, $\frac{1}{\Gamma^2(1-\alpha)(1-2\alpha)}$ becomes larger .

For the case of the Mittag-Leffler kernel,

$$E(t,\alpha) = \int_0^\infty \left(\frac{1}{1-\alpha}\right)^2 E_\alpha\left(-\frac{\alpha}{1-\alpha}t^\alpha\right)^2 dt. \tag{5.6}$$

We recall that for a larger t

$$E_\alpha\left(-\frac{\alpha}{1-\alpha}t^\alpha\right) \approx -\frac{\alpha}{1-\alpha}\frac{t^{-\alpha}}{\Gamma(1-\alpha)} = -\frac{\alpha t^{-\alpha}}{\Gamma(2-\alpha)}. \tag{5.7}$$

Therefore, I have

$$E(t,\alpha) \approx \frac{-\alpha^2}{(1-\alpha)^2\Gamma^2(2-\alpha)}\frac{t^{1-2\alpha}}{(1-2\alpha)}\Big|_\varepsilon^\infty . \tag{5.8}$$

The condition $1-2\alpha < 0$ is needed such that

$$E(t,\alpha) \approx \frac{\alpha^2}{(1-\alpha)^2\Gamma^2(2-\alpha)}\frac{\varepsilon^{1-2\alpha}}{(2\alpha-1)}. \tag{5.9}$$

The energy is finite and is proportional to

$$\frac{\alpha^2}{(1-\alpha)^2\Gamma^2(2-\alpha)}. \tag{5.10}$$

Therefore, when $\alpha \to 0$, the proportional becomes smaller and when $\alpha \to \frac{1}{2}$, the proportional becomes larger.

5.1. Entropy analysis

To calculate the entropy, I should make sure that the functions have density probability [10]. I recall that for a function $f(t)$ to have density probability, it must satisfy the condition

$$\int_0^\infty f(t)\,dt = 1,\ f(t) > 0 \text{ for all } t. \tag{5.11}$$

1. For an exponential law case, I have

$$f(t) = \frac{1}{1-\alpha}\exp\left(-\frac{\alpha}{1-\alpha}t\right), \tag{5.12}$$

and then,

$$\int_0^\infty f(t)\,dt = 1 \Rightarrow \int_0^t \frac{1}{1-\alpha}\exp\left(-\frac{\alpha}{1-\alpha}t\right)dt \tag{5.13}$$

$$= \frac{1}{\alpha}.$$

To obtain 1, I need

$$f_{\alpha}(t) = \frac{\alpha}{1-\alpha}\exp\left(-\frac{\alpha}{1-\alpha}t\right). \tag{5.14}$$

The entropy for the above density is given as

$$\begin{aligned}
H_{\exp}(t,\alpha) &= -\int_0^{\infty}\frac{\alpha}{1-\alpha}\exp\left(-\frac{\alpha}{1-\alpha}t\right)\ln\left(\frac{\alpha}{1-\alpha}\exp\left(-\frac{\alpha}{1-\alpha}t\right)\right)dt \qquad (5.15)\\
&= -\int_0^{\infty}\frac{\alpha}{1-\alpha}\exp\left(-\frac{\alpha}{1-\alpha}t\right)\left[\ln\left(\frac{\alpha}{1-\alpha}\right)-\frac{\alpha}{1-\alpha}t\right]dt\\
&= -\ln\left(\frac{\alpha}{1-\alpha}\right)+\left(\frac{\alpha}{1-\alpha}\right)^2\int_0^{\infty}t\exp\left(-\frac{\alpha}{1-\alpha}t\right)dt\\
&= -\ln\left(\frac{\alpha}{1-\alpha}\right)-\frac{\alpha}{1-\alpha}\left[-\int_0^{\infty}\frac{\alpha}{1-\alpha}t\exp\left(-\frac{\alpha}{1-\alpha}t\right)dt\right]\\
&= -\ln\left(\frac{\alpha}{1-\alpha}\right)-\left(\frac{\alpha}{1-\alpha}\right)\left(\frac{1-\alpha}{\alpha}\right)\\
&= -1-\ln\left(\frac{\alpha}{1-\alpha}\right).
\end{aligned}$$

Then, I have

$$\begin{aligned}
H_{\exp}(t,\alpha) &= \ln\left(\frac{1-\alpha}{\alpha}\right)-1 \qquad (5.16)\\
&= \ln\left(\frac{1-\alpha}{\alpha}\right)+\ln\left(\exp(-1)\right)\\
&= \ln\left(\frac{1-\alpha}{\alpha}\exp(-1)\right)\\
&= \ln\left(\frac{1-\alpha}{\alpha\exp(1)}\right).
\end{aligned}$$

Taking the limit, I have

$$\lim_{\alpha\to 0^+} H_{\exp}(t,\alpha) = \infty \text{ and } \lim_{\alpha\to 1} H_{\exp}(t,\alpha) = -\infty. \tag{5.17}$$

Thus, as $\alpha \to 0$, the entropy $H_{\exp}(t,\alpha)$ diverges to infinity. This indicates that the system has a very high uncertainty, as the probability density becomes concentrated around zero; this leads to a non-deterministic scenario. As $\alpha \to 1$, the entropy $H_{\exp}(t,\alpha)$ diverges negatively, indicating that, the system has a very low uncertainty. The probability density function is concentrated at a single point, which is a deterministic situation.

For the case of power-law, the well-known Pareto distribution is used to obtain the following entropy

$$H_{power}(\alpha) = \ln\left(\frac{\exp\left(1+\frac{1}{\alpha}\right)}{\alpha}\right). \tag{5.18}$$

Therefore, we have

$$\lim_{\alpha\to 0} H_{power}(\alpha) = \infty. \tag{5.19}$$

The entropy is infinite. This helps us understand that, the system is with high uncertainty. This reflects an important diffuse distribution where the probability density becomes increasingly concentrated near smaller values.

$$\lim_{\alpha\to 1} H_{power}(\alpha) = 2. \tag{5.20}$$

The above result indicates that the system has a moderate level of uncertainty. In this case, the density function is spreading out but is not overconcentrated. For the case of Mittag-Leffler, I recall that as $t \to \infty$

$$E_\alpha(-t^\alpha) \approx \frac{t^{-\alpha}}{\Gamma(1-\alpha)}. \tag{5.21}$$

In our case, I will have

$$\frac{\alpha t^{-\alpha}}{(1-\alpha)^2\Gamma(1-\alpha)}. \tag{5.22}$$

Therefore, a similar analysis can be done.

6. Dimensional balance

In general, dimensional balance in a given equation is essential for several reasons [11]. The first reason is the physical interpretation. The balancing ensures that all involved terms have consistent dimension, which is a key to interpreting each component of the model. The second reason could be the model validity and its application to a real-world. When equation dimensions are not balanced, it is an indication that the selected model cannot accurately describe the real world scenario since the fundamental law of physics are violated. The third version could be scaling, unit consistency, parameter calibration, and prediction power. For this last reason, an unbalanced equation dimensionally makes it difficult to calibrate the model parameters based on data. In particular, when dealing with fractional calculus, parameters such dispersion coefficients, advections, and the fractional orders, change the rate and scale of the process. I consider the transport equation present the dimension balancing for different derivatives, and provide some insights of the media in which the transport takes place. An advection-dispersion equation [12] of concentration of $C(x, y, t)$ is

$$\frac{\partial C}{\partial t} + v\frac{\partial C}{\partial x} = D\frac{\partial^2 C}{\partial x^2}. \tag{6.1}$$

Since the derivative is the rate of change, the dimension is balanced since we have $[C]\left[T^{-1}\right]$ on both sides. Indeed, the above is a transport equation in a homogeneous medium. Let us replace $\frac{\partial C}{\partial t}$ by

$$\frac{1}{1-\alpha}\exp\left(-\frac{\alpha}{1-\alpha}t\right) * \frac{\partial C}{\partial t}, \tag{6.2}$$

and

$$\frac{1}{1-\alpha}E_{\alpha}\left(-\frac{\alpha}{1-\alpha}t^{\alpha}\right)*\frac{\partial C}{\partial t}. \tag{6.3}$$

For the Caputo-Fabrizio, I have

$$\frac{1}{1-\alpha}\int_{0}^{t}\exp\left(-\frac{\alpha}{1-\alpha}(t-z)\right)\frac{\partial C}{\partial z}dz+v\frac{\partial C}{\partial x}=D\frac{\partial^2 C}{\partial x^2}. \tag{6.4}$$

Then, we write

$$\left[{}_{0}^{CF}D_{t}^{\alpha}C\right]=\left[\frac{1}{1-\alpha}\right][C]=\frac{[C]}{[T]}. \tag{6.5}$$

The equation is therefore dimensionally balanced. The same is true for Mittag-Leffler case. For the Caputo case, I have

$$\left[{}_{0}^{C}D_{t}^{\alpha}C\right]=\frac{[C]}{[T^{\alpha}]}. \tag{6.6}$$

However, I have $\frac{[v][C]}{[L]}$ for the velocity term and $\frac{[D][C]}{[L^2]}$ for the dispersion term.

Are the dimensions balanced? This will depend on the interpretation and the dimension of $[D]$ and $[v]$ in the chosen medium. First, one needs to recall that the reason for replacing the fractional order is to capture nonlocality due to the heterogeneity of the medium through which the transport is taking place. This is due to the fact that the fractional time captures the complexities of the real-world transport phenomena, in particular, for a system that exhibits significant heterogeneity and anisotropy. The integration of a fractional order permits modeling of various transport behaviors without a need of extensive adjustments to existing equations. Fractional models can indeed describe the anomalous diffusion and non-local transport behaviors frequently observed in contaminated geological formation. The changes of concentration observed as a function of time depend on the structure of the geological information reflected on the dispersion and velocity in the rock-matrix, which does not have the same behavior as that in a fracture and fault.

Let me consider a transport model in heterogeneous media with N features, and M faults, and preferential paths, and the velocity and dispersion can be defined in a way that includes spatial variability. The Dirac-delta function can be used to indicate the position of fractures and faults. For heterogeneous porous media, the Darcy velocity $\overrightarrow{q}(x,y,z)$ at any point (x,y,z) is provided as

$$\overrightarrow{q}(x,y,z)=-\frac{K(x,y,z)}{M}\nabla h. \tag{6.7}$$

- K is the spatially variable hydraulic conductivity tensor.
- M is the fluid viscosity.
- h is the hydraulic head.

Here,

$$\begin{aligned} K(x,y,z) &= K_0(x,y,z)+\sum_{i=1}^{N}K_{f_i}^{i}\delta\left(x-x_{f_i}\right)\delta\left(y-y_{f_i}\right)\delta\left(z-z_{f_i}\right) \\ &\quad+\sum_{j=1}^{M}K_{p}^{j}\delta\left(x-x_{p_j}\right)\delta\left(y-y_{p_j}\right)\delta\left(z-z_{p_j}\right)+\sum_{k=1}^{P}K_{F}^{k}I_{F}^{k}(x,y,z). \end{aligned} \tag{6.8}$$

- $K_0(x,y,z)$ is the baseline hydraulic conductivity.
- $K_{f_i}^i$ is the hydraulic conductivity for fracture i.
- K_p^j is the hydraulic conductivity for fault j.
- K_F^k is the hydraulic conductivity for preferential path k.
- I_F^k is the indicator function defined as

$$I_F^k = \begin{cases} 1, & \text{if in preferential path } k \\ 0, & \text{elsewhere} \end{cases}. \tag{6.9}$$

The dispersion can be defined as

$$\begin{aligned} D(x,y,z) &= D_m + \alpha_L \left|\overrightarrow{q}(x,y,z)\right| + \alpha_T \left(\overrightarrow{q}(x,y,z) - \left(\overrightarrow{q}\cdot\overrightarrow{n}\right)^2\right) \\ &\quad + \sum_{i=1}^{N} D_{f_i}^i \delta\left(x - x_{f_i}\right)\delta\left(y - y_{f_i}\right)\delta\left(z - z_{f_i}\right) \\ &\quad + \sum_{j=1}^{M} D_p^j \delta\left(x - x_{p_j}\right)\delta\left(y - y_{p_j}\right)\delta\left(z - z_{p_j}\right) + \sum_{k=1}^{P} K_F^k I_F^k(x,y,z). \end{aligned} \tag{6.10}$$

The above formulations of dispersion and velocity are steady-state expressions. Here they assume the system has reached a constant state with no explicit time-dependent. However, in many groundwater and transport problems, the systems are transient. In these systems, water, hydraulic head and concentration change over time. Also, in a complex dynamic where concentration impacts dispersion, the dispersion tensor is given by $D(C(x,y,z))$, which helps capture both spatial heterogeneity and concentration variation. Due to these heterogeneities, it is clear that, due to porous media structure of the aquifer, turbulence, classical Darcy law are not applicable; thus,

$$v' = \frac{dx}{dt^\alpha} = \lim_{t\to t_1} \frac{x(t) - x(t_1)}{t^\alpha - t_1^\alpha}. \tag{6.11}$$

Therefore,

$$[v'] = \frac{[L]}{[T^\alpha]}, [D] = \frac{\left[L^2\right]}{[T^\alpha]}. \tag{6.12}$$

Noting that v' is the average velocity in the defined structure and D is the average dispersion. With these arguments, I have that

$${}_0^C D_t^\alpha C + v\frac{\partial C}{\partial x} = D\frac{\partial^2 C}{\partial x^2}. \tag{6.13}$$

The dimensions are evaluated as

$$\begin{aligned} \left[{}_0^C D_t^\alpha C\right] &= \frac{[C]}{[T^\alpha]}, \\ \left[v\frac{\partial C}{\partial x}\right] &= \frac{[L]}{[T^\alpha]}\frac{[C]}{[L]} = \frac{[C]}{[T^\alpha]}, \\ \left[D\frac{\partial^2 C}{\partial x^2}\right] &= [D]\frac{[C]}{[L^2]} = \frac{\left[L^2\right]}{[T^\alpha]}\frac{[C]}{[L^2]} = \frac{[C]}{[T^\alpha]}. \end{aligned} \tag{6.14}$$

Therefore, I have

$$\frac{[C]}{[T^{\alpha-1}][T]} = \frac{[C]}{[T^{\alpha-1}][T]} \Leftrightarrow \frac{[C]}{[T]} = \frac{[C]}{[T]}. \tag{6.15}$$

The equation is balanced therefore, there is no need to state all the parameters.

7. Convolution and geometry interpretation

I present here the convolution of these kernels and their geometry interpretations [5]. I evaluate $K * K$

$$\begin{aligned}\frac{1}{(1-\alpha)^2}\int_0^t \exp\left(-\frac{\alpha}{1-\alpha}(t-\tau)\right)\exp\left(-\frac{\alpha}{1-\alpha}\tau\right)d\tau &= \frac{1}{(1-\alpha)^2}\int_0^t \exp\left(-\frac{\alpha}{1-\alpha}t\right)d\tau \\ &= \frac{1}{(1-\alpha)^2}\exp\left(-\frac{\alpha}{1-\alpha}t\right)t. \end{aligned}\tag{7.1}$$

Taking the limit, I have

$$\lim_{\alpha\to 1}\frac{1}{(1-\alpha)^2}\exp\left(-\frac{\alpha}{1-\alpha}t\right)t = t\delta(t). \tag{7.2}$$

The above result is due to letting $1-\alpha=\varepsilon$,

$$\begin{aligned}\lim_{\alpha\to 1}\frac{1}{(1-\alpha)^2}\exp\left(-\frac{\alpha}{1-\alpha}t\right)t &= \lim_{\varepsilon\to 0}\frac{1}{\varepsilon^2}\exp\left(\frac{1-\varepsilon}{\varepsilon}t\right)t \\ &= t\delta(t),\end{aligned}\tag{7.3}$$

and

$$\lim_{\alpha\to 0}\frac{1}{(1-\alpha)^2}\exp\left(-\frac{\alpha}{1-\alpha}t\right)t = t. \tag{7.4}$$

For the power-law kernel, I have

$$\begin{aligned}\frac{t^{-\alpha}}{\Gamma(1-\alpha)} * \frac{t^{-\alpha}}{\Gamma(1-\alpha)} &= \frac{1}{\Gamma^2(1-\alpha)}\int_0^t (t-\tau)^{-\alpha}\tau^{-\alpha}d\tau \\ &= \frac{1}{\Gamma^2(1-\alpha)}B(1-\alpha,1-\alpha)\,t^{1-2\alpha} \\ &= \frac{t^{1-2\alpha}}{\Gamma(2-2\alpha)}.\end{aligned}\tag{7.5}$$

Taking the limit, I have

$$\lim_{\alpha\to 0}\frac{t^{1-2\alpha}}{\Gamma(2-2\alpha)} = t, \lim_{\alpha\to 1}\frac{t^{1-2\alpha}}{\Gamma(2-2\alpha)} = \delta(t). \tag{7.6}$$

For $E_\alpha\left(-\frac{\alpha}{1-\alpha}t^\alpha\right)$, we have

$$\frac{1}{(1-\alpha)^2}\int_0^t E_\alpha\left(-\frac{\alpha}{1-\alpha}(t-\tau)^\alpha\right)E_\alpha\left(-\frac{\alpha}{1-\alpha}\tau^\alpha\right)d\tau. \tag{7.7}$$

The above expression is analyzed with asymptotic behaviors as $t \to 0$ and $t \to \infty$. When $t \to 0$, I have

$$E_\alpha\left(-\frac{\alpha}{1-\alpha}t^\alpha\right) = 1 - \frac{\alpha}{1-\alpha}t^\alpha. \tag{7.8}$$

Therefore,

$$\begin{aligned}
&\frac{1}{(1-\alpha)^2}\int_0^t E_\alpha\left(-\frac{\alpha}{1-\alpha}(t-\tau)^\alpha\right)E_\alpha\left(-\frac{\alpha}{1-\alpha}\tau^\alpha\right)d\tau \\
&\approx \frac{t}{(1-\alpha)^2}E_{\alpha,2}\left(-\frac{\alpha}{1-\alpha}t^\alpha\right) \\
&-\frac{\alpha}{(1-\alpha)^3}\sum_{j=0}^{\infty}\frac{\left(-\frac{\alpha}{1-\alpha}\right)^j}{\Gamma(aj+1)}\int_0^t (t-\tau)^{\alpha j}\tau^\alpha d\tau \\
&= \frac{t}{(1-\alpha)^2}E_{\alpha,2}\left(-\frac{\alpha}{1-\alpha}t^\alpha\right) \\
&-\frac{\alpha}{(1-\alpha)^3}\sum_{j=0}^{\infty}\frac{\left(-\frac{\alpha}{1-\alpha}\right)^j}{\Gamma(\alpha j+1)}t^{\alpha j+\alpha+1}B(aj+1,\alpha+1)
\end{aligned} \tag{7.9}$$

$$\begin{aligned}
&= \frac{t}{(1-\alpha)^2}E_{\alpha,2}\left(-\frac{\alpha}{1-\alpha}t^\alpha\right) \\
&-\frac{\alpha\Gamma(\alpha+1)}{(1-\alpha)^3}\sum_{j=0}^{\infty}\frac{t^{\alpha j+\alpha+1}}{\Gamma(\alpha j+\alpha+2)}\left(-\frac{\alpha}{1-\alpha}\right)^j \\
&= \frac{t}{(1-\alpha)^2}E_{\alpha,2}\left(-\frac{\alpha}{1-\alpha}t^\alpha\right) - \frac{\alpha t^{\alpha+1}\Gamma(\alpha+1)}{(1-\alpha)^3}E_{\alpha,\alpha+2}\left(-\frac{\alpha}{1-\alpha}t^\alpha\right).
\end{aligned}$$

When $t \to 0$, I have

$$\lim_{\alpha\to 0} K * K = t, \text{ where } K = E_\alpha\left(-\frac{\alpha}{1-\alpha}t^\alpha\right), \tag{7.10}$$

which is similar to the exponential case

$$\lim_{\alpha\to 1} K * K = t\delta(t) - t^3\delta(t)\Gamma(2). \tag{7.11}$$

When $t \to \infty$, I have

$$E_\alpha\left(-\frac{\alpha}{1-\alpha}t^\alpha\right) \approx \frac{\alpha}{1-\alpha}\frac{t^{-\alpha}}{\Gamma(1-\alpha)}. \tag{7.12}$$

Then, I obtain

$$\begin{aligned}
K * K &= \frac{\alpha}{(1-\alpha)^2}\int_0^t E_\alpha\left(-\frac{\alpha}{1-\alpha}(t-\tau)^\alpha\right)\frac{\tau^{-\alpha}}{\Gamma(1-\alpha)}d\tau \\
&= \frac{\alpha}{(1-\alpha)\Gamma(2-\alpha)}\sum_{j=0}^{\infty}\int_0^t \frac{\left(-\frac{\alpha}{1-\alpha}\right)^j}{\Gamma(\alpha j+1)}(t-\tau)^{\alpha j}\tau^{-\alpha}d\tau
\end{aligned} \tag{7.13}$$

$$= \frac{\alpha t^{1-\alpha}}{(1-\alpha)\Gamma(2-\alpha)} \sum_{j=0}^{\infty} \frac{\left(-\frac{\alpha}{1-\alpha}\right)^{j}}{\Gamma(\alpha j+1)} \frac{\Gamma(\alpha j+1)\Gamma(1-\alpha)}{\Gamma(\alpha j-\alpha+2)} t^{\alpha j}$$

$$= \frac{\alpha t^{1-\alpha}\Gamma(1-\alpha)}{(1-\alpha)\Gamma(2-\alpha)} E_{\alpha,2-\alpha}\left(-\frac{\alpha}{1-\alpha}t^{\alpha}\right).$$

Thus, I have

$$\lim_{\alpha\to 0} K * K = 0, \text{ and } \lim_{\alpha\to 1} K * K \text{ undefined.} \tag{7.14}$$

7.1. Convolution and interpretation

In general, the convolution of V and W is given by

$$(V * W)(t) = \int_0^t V(\tau) W(t-\tau) d\tau. \tag{7.15}$$

Geometrically, the above formula is viewed as a process where the function V is spread by the function W over time. Indeed, several interpretations can be provided; for example, this interpretation can be enriched by visualizing how the above integral accumulates overlapping areas when the function V is shifted across the function W. Let us give a detailed breakdown of the geometric interpretation.

(1) The convolution can be interpreted as a sliding overlap of areas. The convolution integral determines the overlapping area between $V(t)$ and $W(t-\tau)$ as the function W shifts to across V. For each t, $(V * W)(t)$ is the integral of the product $V(\tau).W(t-\tau)$. This shows how much V and the shifted version of W align at that time. This implies that the value of $(V * W)(t)$ at any time t is depending on the history of V up to t, weighted by the shape of W.

(2) The convolution can be viewed as weighted smearing since the shape of W determines how much weight is given to each point of V over time. For example, if the function W is a sharp peak like Dirac-delta, then $V * W$ resembles V closely $(f * \delta)(t) = f$. However, if the function W is spread out or the function decays slowly, $V * W$ blurs W, emphasizing or de-emphasizing different parts depending on the shape of W. The operator can be viewed as a cumulative effect with no memory. For instance, if the function W decays slowly, it indicates that past values of V contribute significantly to the convolution at a later time, which captures the idea that the system recalls previous states.

(3) If $V = h'(t)$, then $h'(t) * W(t)$ represents how the rate of change of $h(t)$ interacts with function $W(t)$. In terms of surface, $h'(\tau) * W(t-\tau)$ represents the instantaneous contribution of the rate of change of h at each time τ combined with the weighted effect of function W. The obtained surface can no longer be smooth due to the sharper features if h' has rapid changes. This gives an illustration on how changes in h propagate via W over time. In terms of accumulated area and slope contribution, $h' * W$ provides an insight into how past rates of change accumulate over time, shaping the value of the system. In other terms, it indicates that each instantaneous rate of change in $h(t)$ continues to exert influence over time, distributed by W.

7.2. Modeling a memory with fast decay

The surface $\frac{h'(t)}{1-\alpha} * \exp\left(-\frac{\alpha}{1-\alpha}t\right)$ changes quickly in the z-axis as increases because of the exponential decay. For the case of the power-law kernel, $h'(t) * \frac{t^{-\alpha}}{\Gamma(1-\alpha)}$ models the influence of $h'(t)$ with the power-law decay here, the past values contribute to the current state in proportion to $\frac{(t-\tau)^{-\alpha}}{\Gamma(1-\alpha)}$. This leads to a long-term memory effect, where the influence of the older values τ persists with a slower decay, which contrasts contrast with exponential case. For the Atangana-Baleanu, the convolution represents a memory effect that decays neither too fast nor too slow with a unique distribution of influence over a past value.

In a geometric sense, convolution of the classical derivative with a fractional kernel can be viewed as a combination of localization (capturing the rate of change) and global memory (smoothing effects that take into account the entire history of the function). The resulting operation will typically soften sharp changes in the graph of the function, especially over long distances, and will create a smooth transition between regions, reflecting the fractional memory captured by the kernel.

The following Table 5 provides more information.

Table 5. Interpretation of convolution.

Kernel type	Convolution surface interpretation	Memory effect	Influence of α on memory
Exponential decay	Sharp, steep decay in height of surface	Fast decay memory	α larger: Longer memory α smaller: Short memory
Power-law	Gradient decay with more extended surface	Long-term memory slower decay	α larger: Short memory α smaller: Longer memory
Mittag-Leffler	Intermediate decay neither steep nor gradual	Memory effect between exponential and power-law	α larger: Closer to exponential α smaller: Closer to power-law

8. Mathematical model of the LED degradation lifespan: Fractional kernel

In this section, I attempt to construct a mathematical model for LED light lifespan degradation. A mathematical model of decay or degradation is due to the time-varying lifetime of the LED light, which is effective as it encapsulates many potential and contributory environmental factors that affect the life characteristics of LEDs over time, material properties, and operating conditions in a differential equation. The following is a systematic approach to building such a model depending on how complex and realistic you would want it. I start with the established core variables and assumptions.

LED degradation can be a function of the following factors:

1) Intrinsic aspects: Properties of material, and quality of manufacturing.

2) External factors: Temperature, humidity, chemical exposure, dust, and contamination.

3) Operational aspects: Duty cycle, current variations, seasonal effects.

4) Temporal Factors: Age, cumulative wear, and other out-of-the-ordinary time effects.

In light of these considerations, I introduce a differential equation with convolution terms to represent memory effects in degradation. This approach is the most suitable because it takes into account cumulative damage associated with possibly irreversible changes, in response to variable environmental factors.

Let $L(t)$ lumen output of the LED at time t, with initial lumen $L(0) = L_0$, which is the initial brightness.

- λ is the decay rate factor, changing with respect to temperature and humidity.
- $T(t)$ is the time varying temperature, potentially periodic due to seasonal change.
- H is the humidity at time t, which changes according to the season. Thus, a mathematical model for the degradation lifespan of LED can be given as

$$\frac{dL(t)}{dt} = -\lambda\left(T(t), H(t)\, E(t)\, L(t)\right), \tag{8.1}$$

where accounts for the environmental degradation, dust and pollution of other external effects.

More factors can be added to capture other factors that can lead to a fast degradation. To do this, I add convolution terms. These terms will account for long-term environmental and proportional factors. I now include into the mathematical model kernels that reflect memory effects due to cumulative damage from humidity, temperature, and pollutants. The modified model is given as:

$$\begin{aligned}\frac{dL(t)}{dt} &= -\beta\int_0^t L(\tau)\, K_1 T(t-\tau)\, d\tau - \gamma\int_0^t L(\tau)\, K_2 H(t-\tau)\, d\tau \\ &\quad -\Omega\int_0^t L(\tau)\, K_3 E(t-\tau)\, d\tau.\end{aligned} \tag{8.2}$$

Here, K_i are memory kernels accounting for temperature, environmental factors, and humidity. β and γ can be used to adjust the impact of each factor on LED decay. Since LED performance can be affected due to seasonal cycles in humidity and temperature, $T(t)$ can be defined as

$$T(t) = \overline{T} + T_s \sin\left(\frac{2\pi t}{365}\right), \tag{8.3}$$

where $\overline{T}$ is the yearly average temperature. $H(t)$ can be defined as

$$H(t) = \overline{H} + H_s \sin\left(\frac{2\pi t}{365}\right). \tag{8.4}$$

To account for the off and on, I define

$$D(t) = \begin{cases} 1, & \text{if on} \\ 0, & \text{if off} \end{cases}. \tag{8.5}$$

Indeed, it is known that LED experiences different stress levels at night. The total count gives the time-dependent usage function. In addition to this, the LEDs from batches could have some levels of impurities leading to degradation rate. $L_0 = L_0(1+\varepsilon)$, where ε could be the quality at variations between different batches. We can add the mechanical stress and vibration,

$$M(t) = A\cos(2\pi f t), \tag{8.6}$$

where A is the amplitude factor of vibration and f is the associated frequency. Corrosive effects and environmental pollutants can be represented as cumulative build up

$$P(t) = \Lambda(t) L(t), \tag{8.7}$$

where $\Lambda(t)$ represents a time-varying pollution concentration.

In countries with occasional electrical surges and variation in voltage can also impact LED, leading to degradation

$$V(t) = \overline{V} + \eta(t), \tag{8.8}$$

where $\eta(t)$ stands for noise term. The model can be revised as:

$$\begin{aligned}
\frac{dL(t)}{dt} = & -\beta \int_0^t D(\tau) V(t-\tau) \frac{T(t-\tau)^{-\alpha}}{\Gamma(1-\alpha)} \frac{dL(\tau)}{d\tau} d\tau \\
& -\gamma \int_0^t \frac{V(t-\tau)}{1-\alpha} \exp\left(-\frac{\alpha}{1-\alpha} H(t-\tau)\right) L(\tau)\, d\tau \\
& -\Omega \int_0^t \frac{V(t-\tau)}{1-\alpha} E_\alpha\left(-\frac{\alpha}{1-\alpha} E(t-\tau)^\alpha\right) L(\tau)\, d\tau \\
& -\varepsilon \Lambda(t) V(t) L(t) \\
& -\xi \int_0^t \frac{V(t-\tau)}{\Gamma(1-\alpha)} M(t-\tau)^{-\alpha} L(\tau)\, d\tau.
\end{aligned} \tag{8.9}$$

The table below is a summary of the model. Each term's physical interpretation is presented in Table 6.

Table 6. Physical meaning of model.

Components	Physical meaning
$-\beta\int\limits_0^t D(\tau)\,V(t-\tau)\,\frac{T(t-\tau)^{-\alpha}}{\Gamma(1-\alpha)}\frac{dL(\tau)}{d\tau}d\tau$	Duty cycle and thermal decay, modulated by voltage fluctuations
$-\gamma\int\limits_0^t \frac{V(t-\tau)}{1-\alpha}\exp\left(-\frac{\alpha}{1-\alpha}H(t-\tau)\right)L(\tau)\,d\tau$	Humidity, environmental degradation due to electrical fluctuations
$-\Omega\int\limits_0^t \frac{V(t-\tau)}{1-\alpha}E_\alpha\left(-\frac{\alpha}{1-\alpha}E(t-\tau)^\alpha\right)L(\tau)\,d\tau$	Decay due to aging under voltage and structural stress
$-\varepsilon\Lambda(t)\,V(t)\,L(t)$	Decay due to pollution, influenced by electrical stress
$-\xi\int\limits_0^t \frac{V(t-\tau)}{\Gamma(1-\alpha)}M(t-\tau)^{-\alpha}L(\tau)\,d\tau$	Decay due to vibration, and mechanical stress

The solution of the above model can be given numerically

$$\begin{aligned}\frac{L^{n+1}-L^n}{\Delta t} &= -\beta\int\limits_0^{t_{n+1}} D(\tau)\,V(t_{n+1}-\tau)\,\frac{T(t_{n+1}-\tau)^{-\alpha}}{\Gamma(1-\alpha)}\frac{dL(\tau)}{d\tau}d\tau \\ &\quad -\gamma\int\limits_0^{t_{n+1}}\frac{V(t_{n+1}-\tau)}{1-\alpha}\exp\left(-\frac{\alpha}{1-\alpha}H(t_{n+1}-\tau)\right)L(\tau)\,d\tau \\ &\quad -\Omega\int\limits_0^{t_{n+1}}\frac{V(t_{n+1}-\tau)}{1-\alpha}E_\alpha\left(-\frac{\alpha}{1-\alpha}E(t_{n+1}-\tau)^\alpha\right)L(\tau)\,d\tau \\ &\quad -\varepsilon\Lambda(t_{n+1})\,V(t_{n+1})\,L(t_{n+1}) \\ &\quad -\xi\int\limits_0^{t_{n+1}}\frac{V(t_{n+1}-\tau)}{\Gamma(1-\alpha)}M(t_{n+1}-\tau)^{-\alpha}L(\tau)\,d\tau \end{aligned} \tag{8.10}$$

$$\begin{aligned} &= -\beta\sum_{j=0}^{n}\int\limits_{t_j}^{t_{j+1}} D(\tau)\,V(t_{n+1}-\tau)\,\frac{T(t_{n+1}-\tau)^{-\alpha}}{\Gamma(1-\alpha)}\frac{dL(\tau)}{d\tau}d\tau \\ &\quad -\gamma\sum_{j=0}^{n}\int\limits_{t_j}^{t_{j+1}}\frac{V(t_{n+1}-\tau)}{1-\alpha}\exp\left(-\frac{\alpha}{1-\alpha}H(t_{n+1}-\tau)\right)L(\tau)\,d\tau \end{aligned}$$

$$-\Omega \sum_{j=0}^{n} \int_{t_j}^{t_{j+1}} \frac{V(t_{n+1}-\tau)}{1-\alpha} E_\alpha \left(-\frac{\alpha}{1-\alpha} E(t_{n+1}-\tau)^\alpha\right) L(\tau)\, d\tau$$
$$-\varepsilon \Lambda (t_{n+1}) V(t_{n+1}) L(t_{n+1})$$
$$-\xi \sum_{j=0}^{n} \int_{t_j}^{t_{j+1}} \frac{V(t_{n+1}-\tau)}{\Gamma(1-\alpha)} M(t_{n+1}-\tau)^{-\alpha} L(\tau)\, d\tau.$$

To simplify the scheme, I can approximate

$$M(t) = A, E(t) = \overline{E} \pm \Delta E, H(t) = \overline{H} \pm \Delta H_s, T(t) = \overline{T} \pm \Delta T_s, V(t) = \overline{V} \pm V_s. \tag{8.11}$$

The numerical solution is

$$\begin{aligned} \frac{L^{n+1}-L^n}{\Delta t} &= -\beta\left(\overline{V} \pm V_s\right) \frac{\left(\overline{T} \pm \Delta T_s\right)^{-\alpha}}{\Gamma(1-\alpha)} \sum_{j=0}^{n} D\left(t_j\right) \frac{L^{j+1}-L^j}{\Delta t} \Delta t \\ &\quad -\gamma \exp\left(-\frac{\alpha}{1-\alpha} H(t_{n+1}-\tau)\right) \frac{\left(\overline{V} \pm V_s\right)}{1-\alpha} \sum_{j=0}^{n} L\left(t_j\right) \Delta t \\ &\quad -\Omega \frac{\left(\overline{V} \pm V_s\right)}{1-\alpha} \sum_{j=0}^{n} E_\alpha \left(-\frac{\alpha}{1-\alpha} \left(\overline{E} \pm \Delta E\right)^\alpha\right) L\left(t_j\right) \Delta t \\ &\quad -\varepsilon \Lambda (t_{n+1}) V(t_{n+1}) L(t_{n+1}) \\ &\quad -\xi A^{-\alpha} \frac{\left(\overline{V} \pm V_s\right)}{\Gamma(1-\alpha)} \sum_{j=0}^{n} L\left(t_j\right) \Delta t. \end{aligned} \tag{8.12}$$

9. Conclusions

The power of fractional calculus in accurately capturing the essential time-dependent behaviors of systems with non-trivial memory is exemplified. In particular, I have presented an extensive analysis of the Caputo-Fabrizio and Atangana-Baleanu fractional derivatives to illustrate how the fractional order can serve as a time dimension with rich memory signatures that integer-order calculus cannot accommodate. As discussed in terms of kernel properties, memory effects, energy dynamics, and convolution geometry, the fractional derivatives that produce these functions facilitate deeper levels of agreement with real-world physics. The LED lifespan model elaborated in this paper is an example of the practical use of fractional calculus. This model uses several fractional kernels, including exponential, power law, and the Mittag-Leffler kernels, which can efficiently describe the differential effects of electrical, mechanical, and environmental stressors on LED degradation, to provide a more precise prediction of LED life. This is an important step toward the broader applicability of fractional derivatives in various fields, showing that not only is there a sound theory behind fractional calculus but it also holds potential as a practical tool for solving real-life engineering and scientific problems.

Use of Generative-AI tools declaration

The author declares he has not used Artificial Intelligence (AI) tools in the creation of this article.

Conflict of interest

Author declares no conflict of interest.

References

1. I. Podlubny, *Fractional differential equations*, vol. 198 of Mathematics in Science and Engineering, San Diego: Academic Press, 1999,
2. H. R. Blank, M. Frank, M. Geiger, J. Heindl, M. Kaltenhäuser, W. Kreische, et al., Dimension and entropy analysis of MEG time series from human α-rhythm, *Z. Phys. B-Condens. Matter*, **91** (1993), 251–256. https://doi.org/10.1007/BF01315243
3. M. Caputo, M. Fabrizio, A new definition of fractional derivative without singular kernel, *Prog. Fract. Differ. Appl.*, **1** (2015), 73–85.
4. A. Atangana, D. Baleanu, New fractional derivatives with non-local and non-singular kernel: Theory and application to heat transfer model, thermal science, *arxiv preprint*, 2016.
5. B. Deng, R. Tao, Y. Wang, Convolution theorems for the linear canonical transform and their applications, *Sci. China Ser. F*, **49** (2006), 592–603. https://doi.org/10.1007/s11432-006-2016-4
6. W. Chen, Time-space fabric underlying anomalous diffusion, *Chaos Soliton. Fract.*, **28** (2006), 923–929. https://doi.org/10.1016/j.chaos.2005.08.199
7. A. Atangana, Fractal-fractional differentiation and integration: Connecting fractal calculus and fractional calculus to predict complex system, *Chaos Soliton. Fract.*, **102** (2017), 396–406. https://doi.org/10.1016/j.chaos.2017.04.027
8. K. X. Li, J. G. Peng, Laplace transform and fractional differential equations, *Appl. Math. Lett.*, **24** (2011), 2019–2023. https://doi.org/10.1016/j.aml.2011.05.035
9. D. A. Gomes, J. B. Jimenez, T. S. Koivisto, Energy and entropy in the geometrical trinity of gravity, *Phys. Rev. D*, **107** (2023). https://doi.org/10.1103/PhysRevD.107.024044
10. R. Anttila, Local entropy and Lq-dimensions of measures in doubling metric spaces, *PUMP J. Undergrad. Res.*, **3** (2020), 226–243. https://doi.org/10.46787/pump.v3i0.2434
11. C. A. Poveda, The theory of dimensional balance of needs, *Int. J. Sustain. Dev. World*, **24** (2016), 97–119. https://doi.org/10.5553/TCR/092986492016024004001
12. D. A. Benson, S. W. Wheatcraft, M. M. Meerschaert, Application of a fractional advection-dispersion equation, *Water Resour. Res.*, **36** (2000), 1403–1412. https://doi.org/10.1029/2000WR900031